JOURNAL OF AGRICULTURAL AND FOOD CHEMISTRY

Proteomic Analysis of Caco-2 Cells Treated with Monacolin K

WUN-YUAN LIN,† CHING-YUNG SONG,† AND TZU-MING PAN*,‡

Institute of Microbiology and Biochemistry, National Taiwan University, Taipei, Taiwan, and Department of Food Science, Nutrition and Nutraceutical Biotechnology, Shih Chien University, Taipei, Taiwan, Republic of China

Monascus species is an important traditional fermentation fungus used on food. Monacolin K (a secondary metabolite of *Monascus*, a competitive inhibitor of 3-hydroxy-3-methylglutaryl coenzyme A reductase) in inhibition of mevalonate synthesis may result in reductions of isoprenoid prenylation in cells. Impairment of protein isoprenoid prenylation has been related to anticancer effect in cancer cells. As a functional food for *Monascus*, however, the molecular mechanisms responsible for the anti-proliferate effect of monacolin K in cancer cells are not clear. We used proteomic analysis by two-dimensional gel electrophoresis, matrix-assisted laser desorption ionization time-of-flight/time-of-flight mass spectrometry (MALDI-TOF/TOF MS), tandem mass spectrometry (MS/MS), and database interrogation to separate and identify the proteins of Caco-2 cells treated with monacolin K. The results showed that monacolin K inhibited the proliferation of Caco-2 cells in a dose-dependent manner. The identified proteins in proteomic analysis included anti-oxidation enzymes related to reactive oxygen species stress, cytoskeleton proteins, glycolytic enzymes, and enzymes involved in mediating protein interactions. Furthermore, glutathione S-transferase P 1 and cytoskeleton-8, -18, and -19 revealed a down-regulation in a dose-dependent manner in exposure of Caco-2 cells to monacolin K.

KEYWORDS: ***Monascus*; monacolin K; anti-cancer; proteomics**

INTRODUCTION

It is well-known that *Monascus* species is a traditional fermentation fungus used on food in Asia for centuries. The types of secondary metabolites produced from *Monascus* species include an antihypercholesterolemic agent (monacolin K), pigments, antioxidant compounds (dimerumic acid among others), and an antibacterial activity compound (citrinin) (*1*−*4*). Monacolin K (MK, an analog of lovastatin and mevinolin) is a competitive inhibitor of 3-hydroxy-3-methylglutaryl coenzyme A (HMG-CoA) reductase that reduces cholesterol synthesis by blocking the conversion of HMG-CoA to mevalonate (*5*). Inhibition of mevalonate synthesis may also result in reductions of isoprenoid prenylation, including geranylgeranyl pyrophosphate and farnesyl pyrophosphate (*6*). Prenylation of small GTP-binding proteins, such as Ras superfamily proteins, with a farnesyl or geranylgeranyl group, is required for their translocation to the plasma membrane and their functions (*7*−*9*). Translocation of small GTP-binding proteins is related to cell survival, proliferation, and differentiation (*9*, *10*).

The clinical use of red mold rice (*Monascus*-fermented rice) has revealed effect in lowering plasma cholesterol levels (*3*, *11*). However, the use of natural food dietary agents is being increasingly appreciated as an effective method for the management of many cancer types in an approach known as cancer chemoprevention for many years (*4*). HMG-CoA reductase inhibitors have been observed in inhibition in cellular proliferation and induction of apoptosis in several experimental systems, making them potential anticancer agents (*12*, *13*). The fact that red mold rice containing MK may be used as an anticancer agent makes it more popular in the development of functional health food. Previous studies implicated that by limiting mevalonate bioavailability, HMG-CoA reductase inhibitor may influence not only the cholesterol levels but also the expression of several proteins (*12*, *14*). Although inhibition of these GTP-binding proteins by impairment of protein isoprenylation has been related to its anticancer effect in cancer cells, the molecular mechanisms responsible for the anti-proliferative effect of HMG-CoA reductase inhibitors are not clear.

Based on high-resolution two-dimensional electrophoresis (2-DE) and mass spectrometry, proteomics is a powerful tool for analysis of hundreds proteins expressed in a complex mixture at one time (*15*). The proteome provides a better understanding of dynamic and overall view of the cell machinery under various conditions. The objective of this work was to use proteomic analysis to identify the proteins of Caco-2 colorectal adenocarcinoma cells, a well established *in vitro* model in evaluation of nutrient absorption (*16*, *17*), treated with MK and examine the protein profiles related to the MK-induced anti-proliferative effect. In this study, a total of 17 proteins were uncovered with

* Author to whom correspondence should be addressed. Telephone: +886-2-3366-4519. Fax: +886-2-2362-7044. E-mail: tmpan@ntu.edu.tw.
† Shih Chien University.
‡ National Taiwan University.

10.1021/jf061060c CCC: $33.50
Published on Web 08/02/2006

a more than 1.3-fold expression in exposure of 75 μM MK to Caco-2 cells.

MATERIALS AND METHODS

Reagents and Materials. The electrophoresis reagents including acrylamide solution (25%), urea, thiourea, 3-[(3-cholamidopropyl) dimethylammonio]-1-propane sulfonate (CHAPS), dithiothreitol (DTT), Immobilline Dry Strips, immobilized pH gradients (IPG) buffer, IPG cover mineral oil, Tris base, sodium dodecyl sulfate (SDS), iodoacetamide (IAA), trifluoroacetic acid (TFA), and protein assay kit were purchased from Bio-Rad (Hercules, CA). Monacolin K (MK), 3-(4,5-dimethyl thiazol-2-yl)-2,5-diphenyl tetrazolium bromide (MTT), dimethyl sulfoxide (DMSO), and α-cyano-4-hydroxycinnamic acid (CHCA) were purchased from Sigma (St. Louis, MO). Sypro Ruby stain was purchased from Amersham Biosciences (Piscataway, NJ). Trypsin (modified) was obtained from Promega (Madison, WI). ZipTip C_{18} microcolumns were purchased from Millipore (Bedford, MA). Mouse monoclonal antibodies for anti-cytoskeletal 8/18, anti-cytoskeletal 19, anti-glutathione S-transferase P1, and anti-β-actin were purchased from Lab Vision (Fremont, CA). Anti-c-Myc and goat-anti-mouse IgG horseradish peroxidase-conjugated secondary antibodies were purchased from BD Biosciences (Franklin Lakes, NJ).

Cell Culture. The human colorectal adenocarcinoma cells, Caco-2 cell line (BCRC 60182), were obtained from the Bioresource Collection and Research Center (BCRC) in Taiwan and were cultured in minimal essential medium (MEM; Gibco BRL, Grand Island, NY) supplemented with 10% fetal bovine serum (Biochrom AG, Berlin, Germany), 44 mM sodium bicarbonate (Sigma), 100 U/mL penicillin, and 100 μg/mL streptomycin (Gibco BRL) antibiotics at 37 °C under 5% CO_2 and 95% air. For treatment with MK, cells were cultured in MEM until nearly confluent. Medium was removed and replaced by a medium containing either the solvent DMSO or various concentrations of MK (solubilized in DMSO). Cells were then harvested at the times stated in the figure legends.

MTT Reduction Assay and Morphological Observation. The cytotoxic effect of MK against Caco-2 cells was determinated by the MTT assay. The MTT assay is based on the reduction of the MTT by viable cells. Briefly, Caco-2 cells (1×10^5/cm^2) were incubated in 96-well microtiter plates. After treatment with various concentrations of MK (0−200 μM) for 24 and 48 h, 50 μL of MTT solution (1 mg/mL in PBS) was added to each well, and the plates were incubated for an additional 4 h at 37 °C. MTT solution in medium was aspirated off. To achieve solubilization of the purple-blue MTT formazan crystals formed in viable cells, 200 μL of DMSO was added to each well. The absorbance was read at 595 nm on a microtiter plate ELISA reader (MRX-reader, DYNEX Technologies, Chantilly, VA) with DMSO as the blank. The appearance of morphologic change was assessed after exposure of 5, 25, and 75 μM MK for 48 h, being viewed on an inverted light microscope (IX 70, Olympus, Tokyo, Japan).

Sample Preparation and Two-Dimensional Electrophoresis. The cells were trypsinized and washed with PBS buffer. The cells were diluted with lysis buffer (7 M urea, 2 M thiourea, 4% w/v CHAPS, and 0.002% bromophenol blue). After sonication, the protein pellet was solubilized completely in sample buffer (7 M urea, 2 M thiourea, 4% w/v CHAPS, 65 mM DTT, and 0.5% IPG buffer with a trace of bromophenol blue) and left to stand for 1 h at 4 °C. After 10 min of centrifugation at 18 000 × *g* at 4 °C, 350 μL of supernatant containing 300 μg of proteins were loaded onto the IPG strip. Protein content was determined by the Bradford method (protein assay kit; Bio-Rad). Isoelectric focusing (IEF) was carried out *via* a stepwise voltage increment with the following conditions: step 1 rehydration, 10 V for 12 h; step 2, 100 V for 1 h; step 3, 250 V for 1 h; step 4, 500 V for 1 h; step 5, 1000 V for 1 h; step 6, 4000 V for 1 h; step 7, 8000 V for 45 kVh; total, 50 975 Vh. Following IEF separation, the gel strip was first equilibrated for 15 min in equilibration buffer containing 50 mM Tris (pH 8.8), 6 M urea, 30% v/v glycerol, 2% w/v SDS, and 2% w/v DTT and subsequently in the same buffer with 2.5% w/v IAA replacing DTT for another 15 min. The equilibrated strip was then transferred onto the second-dimension SDS−PAGE gel and sealed in place with 0.5% agarose. SDS−PAGE was performed on 10−18% gradient polyacrylamide gel (18.5 cm × 18.5 cm × 1.5 mm) at a constant voltage of 10 mA for 0.25 h and 45 mA for 3.5 h until the dye front reached the bottom of the gel. Sypro Ruby stain was used for visualization of the 2-DE gel. The fluorescence-stained 2-DE gel was digitally scanned as a 2-DE image on the Typhoon 9200 fluorescence image scanner (Amersham Biosciences). Spot detection, quantification, and matching were managed using PDQuest software (Bio-Rad). The theoretical molecular mass (M_r) and p*I* values of the 2-DE markers were used to calibrate the M_r and p*I* of the protein spots in the 2-DE gels. Intensity levels were normalized between gels as a proportion of the total protein intensity detected for the entire gel, and protein quantity of each spot was calculated by integrating the density over the spot area.

In-Gel Tryptic Digestion. The protein spots detected on 2-DE were manually excised from the gel and cut into pieces. The pieces were then washed twice with 50% acetonitrile (ACN) in 25 mM ammonium bicarbonate, pH 8.5, for 15 min each time, dehydrated with 100% ACN for 5 min, dried, and rehydrated with a total of 100 ng of sequencing grade, modified trypsin in 25 mM ammonium bicarbonate, pH 8.5, at 37 °C for 16 h. Following digestion, tryptic peptides were extracted twice with 50% ACN containing 5% formic acid for 15 min each time with moderate sonication. The extracted solutions were pooled and evaporated to dryness under vacuum. Dry peptide samples were redissolved in 0.1% TFA and purified by ZipTip C_{18} microcolumns according to the manufacturer's instruction manual, where necessary.

MALDI-TOF/TOF. MALDI-MS detection and MS/MS sequencing of isopeptides in reflectron mode were performed on an Applied Biosystems 4700 Proteomics Analyzer mass spectrometer (Applied Biosystems, Framingham, MA) equipped with an Nd:YAG laser (355 nm wavelength, <500-ps pulse, and 200 Hz repetition rate in both MS and MS/MS modes). A total of 1000 and 2500 shots were accumulated in positive ion mode MS and MS/MS modes, respectively. The tryptic digested peptide samples were dissolved in 50% ACN with 0.1% formic acid and premixed with a 5 mg/mL matrix solution of CHCA in 70% ACN with 0.1% formic acid for spotting onto target plate. For collision-induced dissociation (CID) MS/MS operation, the indicated collision cell pressure was increased from 3.0×10^{-8} Torr (no collision gas) to 5.0×10^{-7} Torr, with the potential difference between the source acceleration voltage and the collision cell set at 1 kV. The resolution of timed ion selector for precursor ion was set at 200. MS data was acquired using the instrument internal calibration. At a resolution above 10 000 in MS mode, accurate mass measurement (<50 ppm) of the monoisotopic isopeptide signals is possible. MS/MS data was acquired using the instrument default calibration.

Data Search. After data acquisition, the files were searched by querying the SwissProt or NCBI database or both using MASCOT (http://www.matrixscience.com) with the following parameters: peptide mass tolerance, 50 ppm; MS/MS ion mass tolerance, 0.25 Da; allow up to one missed cleavage; variable modifications considered were methionine oxidation and cysteine carboxyamidomethylation; taxonomy to human source.

Western Blotting. For Western blotting, Caco-2 cells were cultured with 0, 5, 25, and 75 μM MK for 48 h. Cells were washed with PBS and lysed in sample buffer (0.0625 M Tris-HCl, 2% SDS, 10% glycerol, 0.1 M DTT, and 0.01% bromophenol blue). Protein concentration was also determined by the Bradford method using protein assay kit (Bio-Rad). Equal amounts of protein were separated on 8−12% SDS−polyacryamide gel, transferred onto nitrocellulose membranes, blocked with TBST (Tris-buffered saline, pH 7.4, and 0.05% Tween-20) with 5% nonfat milk. The following antibodies were used as primary antibodies for 2 h incubation: mouse monoclonal anti-β-actin (diluted at 1:3000), anti-cytoskeletal 8/18 (1:3000), anti-cytoskeletal 19 (1:3000), anti-glutathione S-transferase P1 (1:100), and anti-c-Myc (1:1000). After the next washing, membranes were incubated for 1 h with the horseradish peroxidase-conjugated secondary antibodies (1:10 000) and washed with TBST, the color reaction was developed using a chemoluminescence detection kit (ECL; Amersham Biosciences) following the manufacture's instruction, and the films were analyzed using software ImageQuant (Molecular Dynamics, Inc., Sunnyvale, CA).

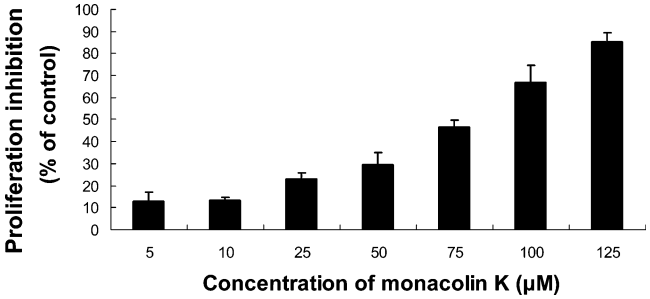

Figure 1. Effect of monacolin K on proliferation inhibition of Caco-2 cells. Cells were treated for 48 h with the indicated concentrations of monacolin K. Cell proliferation inhibition was assessed by MTT assay as described in Materials and Methods. The data shown are the means (percentage of control) ± SEM from three independent experiments.

RESULTS

The Cytotoxic Effect and Morphologic Changes on Caco-2 Cells after MK Exposure. We first examined the cytotoxic effect of MK on Caco-2 cells by using an MTT reduction assay, the mechanism of MTT assay is that a colorless tetrazolium salt is cleaved and converted to a blue formazan by mitochondrial dehydrogenases of living cells (*18*, *19*). Following *in vitro* treatment of the cells with increasing concentrations of MK (0−200 μM) for 24 and 48 h, respectively, the results showed that the cell proliferation was inhibited in a dose-dependent manner after MK exposure (**Figure 1**). The IC_{50} of MK on Caco-2 cell proliferation was ∼75 μM (30.3 mg/kg). In comparison, in a clinical phase II trial investigating the potential value of lovastatin (a MK analog) to be administered for patients with advanced gastric adenocarcinoma, clinical responses required oral dosages of 35 mg/(kg body·day) (*3*, *20*). However, when *Monascus* products are defined as functional health food, cholesterol-lowering products called Red Mold Rice (*M. purpurus* rice) sold as dietary supplements in Asia contain 1−1.5% w/w MK, and in our previous study, the MK production in *Monascus* powder (*M. purpureus* NTU 568) of oral administration for hyperlipidemia hamster was 9500 mg/kg (*21*). Furthermore, the morphologic features in changes of the treated cells were observed through an inverted light microscopy. The untreated Caco-2 cells grew in a monolayer and smoother surface manner (**Figure 2A**). It was observed that exposure of 5, 25, and 75 μM MK to the cells for 24 (figures not shown) and 48 h induced morphological changes that involved cell shrinkage and cytoplasmic vaculation (**Figure 2B−D**).

Protein Separation and Identification. Since the induction of cytotoxic effect of MK on Caco-2 cells was better after 48 h exposure than after 24 h exposure, 2-DE gels of the cells treated with MK for 48 h were prepared and identified with proteomic technology. Proteins were extracted directly from cultured cells with urea lysis solution and resolved by 2-DE using IPG (linear) ranging from p*I* 3−10 to separate the extracted proteins. 2-DE analysis is a multistep technique strongly dependent on several factors such as sample application, quality of gels for the second dimension, and staining duration. Therefore, the most pressing problem is image registration, which ensures that identical proteins in different gels are recognized as being identical. With registration of several gel images, a single reference or consensus gel image that combines the information content of all individual images was generated. In this study, this reference gel consisted of a representative set of spots generated from repeatedly four registered gel images of the control cells (untreated) or MK-treated cells and was used to compare each sample. Approximately 500 protein spots were visualized on each 2-DE gel (18 cm × 18 cm) by staining with Sypro Ruby. **Figures 3** and **4** display the proteome profilings of the control cells and the representative pair of protein spots for the control cells versus the MK-treated cells. Around 100 protein spots were revealed to have altered expressions between the treatments on the 2-DE gel according to image analysis using software PDQuest program (Bio-Rad), excised, and subjected to in-gel tryptic digestion, MALDI-TOF/TOF-MS, and peptide mass fingerprints (PMF) to obtain protein identification by database search. In cases that PMF alone was not sufficient for

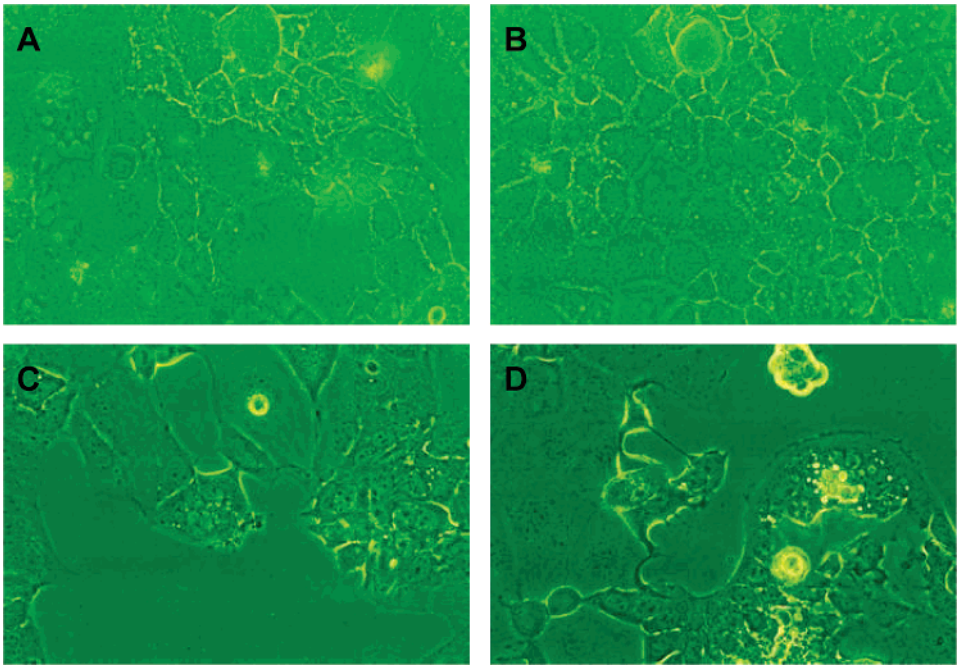

Figure 2. Caco-2 cell morphological changes were observed through an inverted light microscope (IX70, Olympus) under 400× magnification after treatment with monacolin K for 48 h under the following conditions: (**A**) control cells; (**B**) 5 μM monacolin K; (**C**) 25 μM monacolin K; (**D**) 75 μM monacolin K.

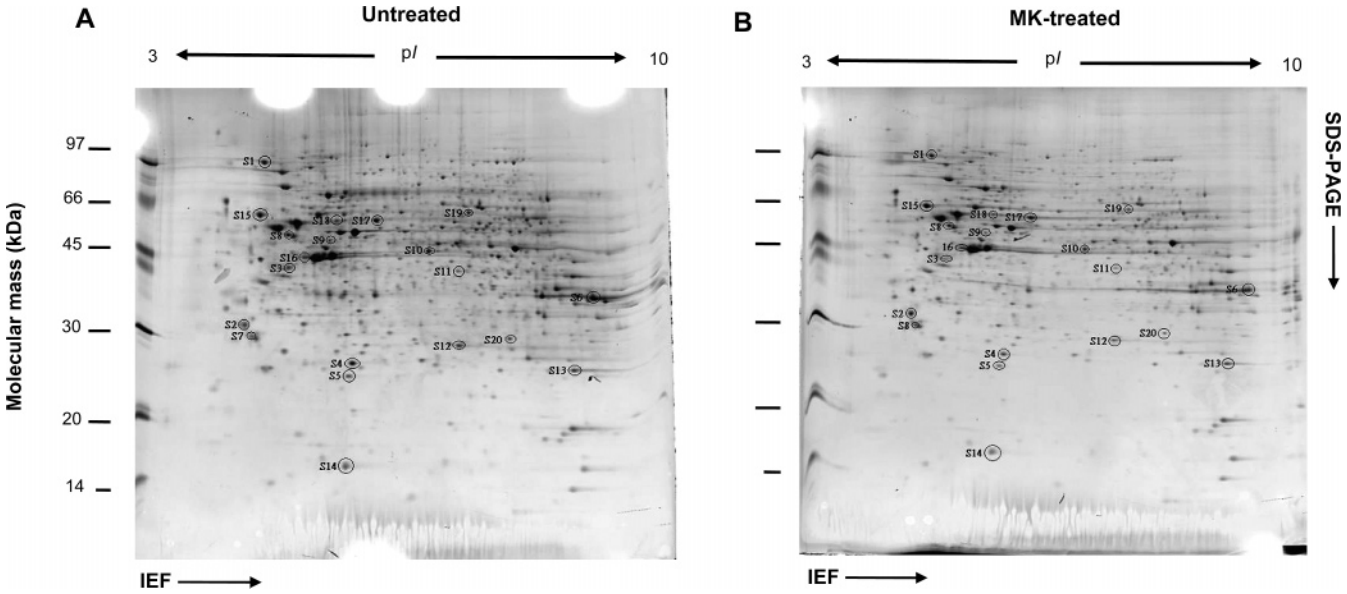

Figure 3. 2-DE gel maps of Caco-2 cells derived from the untreated control (**A**) and treatment with monacolin K for 48 h (**B**). The protein (300 μg/350 μL) was applied to pH 3–10 linear IPG strips (18 cm), using 10–18% vertical linear gradient SDS–PAGE as the second dimension. The gel was visualized by Sypro Ruby staining. Protein spots marked on the maps represent 20 identified proteins with differential expression after monacolin K treatment in analysis. Details of the proteins are given in **Table 1**.

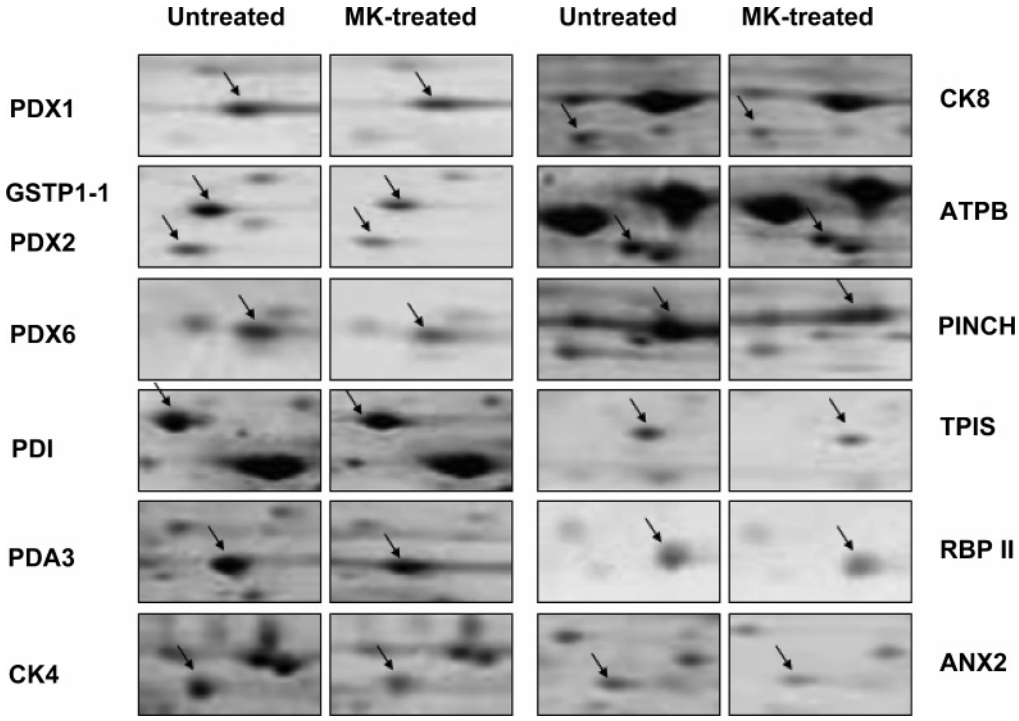

Figure 4. Enlarged view of detailed alteration patterns of the 13 representative protein spots from 2-DE gel maps in **Figure 3** (differentially expressed between the untreated and monacolin K-treated Caco-2 cells).

identification, proteins were identified subsequently by MS/MS analysis of specific precursor ions. Results are summarized in **Table 1**, listing the identified 20 proteins, together with corresponding spot numbers, theoretically predicted M_r and p*I* values, peptides matched, SwissProt scores, and accession numbers of identified proteins.

Protein Expression Alterations in Caco-2 Cells after MK Exposure. The altered expression proteins distributed throughout the entire gels (**Figures 3** and **4**), indicating that multiple clusters of proteins are involved in the process of cytotoxity of MK on Caco-2 cells. Seventeen protein spots among the identified proteins were detected to be more than 1.3-fold deregulated in four independent experiments (**Table 1**). Among them, 15 were down-regulated and only two were up-regulated in the MK-treated cells compared to the control cells. Some of these proteins may be classified into several categories based on their functions, including anti-oxidation enzymes related to reactive oxygen species (ROS) stress, cytoskeleton proteins, glycolytic enzymes, and enzymes involved in mediating protein interactions. The ROS stress-related enzymes that were down-regulated in the MK-treated cells included glutathione S-transferase P1 (GSTP1-1), peroxiredoxin 1 (PDX 1), thioredoxin-dependent peroxide reductase 1 (PDX 2), and peroxiredoxin 6 (PDX 6). Three identified cytoskeletal (CK) proteins (CK 4,

Table 1. List of Identified Protein Spots Differentially Expressed between the Untreated and Monacolin K-Treated Caco-2 Cells, Identified by PMF and Subsequent MS/MS Analysis

spot no.	protein identified (M_r/pI)[a]	peptides matched	sequence coverage (%)[b]	accession no.[c]	identification[d]	MOWSE score	fold change	MS/MS sequence
S1	endoplasmin precursor (ENPL) (92 kDa/4.76)	9	14	P14625	PMF	65	−1.4	
S2	Cohen syndrome protein 1 (COH1) (32 kDa/4.79)	7	27	Q7Z7G8-04-00-0	PMF	42	−5.5	
S3	type I cytoskeletal 19 (CK 19) (44 kDa/5)	13	45	P08727-00-00-00	MSMS	37	−2.9	FGPGVAFRAPSI HGGSGGR
S4	glutathione S-transferase P 1 (GSTP1-1) (23 kDa/5.4)	5	32	P09211-00-00-00	MSMS	250	−1.4	PPYTVVYFPVR FQDGDLTLYQSN TILRALPGQLKPF ETLLSQNQGGK
S5	thioredoxin- dependent peroxide reductase 1 (PDX 2) (21 kDa/5.7)	7	29	P32119	MSMS	47	−2.5	KEGGLGPLNIPL LADVTR
S6	particularly interesting new Cys-His protein (PINCH) (37 kDa/8.4)	9	20	P48059	PMF	32	−2	
S7	protein kinase C inhibitor protein-1 (KCIP-1) (27 kDa/4.7)	9	43	P63104	PMF	92	−1.2	
S8	ATP synthase β chain (ATPB) (56 kDa/5.3)	13	42	P06576	MSMS	185	−3.6	FTQAGSEVSALLGR LVLEVAQHLGESTVR
S9	type II cytoskeletal 8 (CK 8) (53 kDa/5.5)	19	27	P05787	MSMS	181	−1.9	FASFIDKVR LALDIEIATYR LQAEIDALKGQR
S10	non-neural enolase (ENOA) (47 kDa/7)	13	35	P06733	MSMS	129	−1.5	AGYTDKVVIGMD VAASEFFR YNQLLRIEEELGSK NFRNPLAK
S11	annexin A2 (ANX 2) (38 kDa/7.6)	12	39	P07355-00-00-00	MSMS	42	+2	AYTNFDAERDAL NIETAIK
S12	peroxiredoxin 6 (PDX 6) (24 kDa/6	8	46	P30041	MSMS	138	−1.4	VVISLQLTAEKR PGGLLLGDVAPN FEANTTVGR
S13	peroxiredoxin 1 (PDX 1) (22 kDa/8.3)	2	11	Q06830	MSMS	53	−2.2	QITVNDLPVGR GLFIIDDKGILR
S14	retinoic acid-binding protein II (RBP II) (15 kDa/5.4)	2	33	P29373	MSMS	63	+1.3	IAVAAASKPAVEI KQEGDTFYIK TTEINFKVGEEF EEQTVDGRPCK
S15	protein disulfide isomerase precursor (PDI) (57 kDa/4.8)	15	37	P07237	MSMS	82	−1.5	ILFIFIDSDHTDNQR FFPASADRTVIDYNG ER
S16	heterogeneous nuclear ribonucleoprotein K (ROK) (50 kDa/5.4)	2	2	P61978-00-00-00	MSMS	61	+1.1	NLPLPPPPPPR
S17	protein disulfide isomerase A3 precursor (PDA 3) (55 kDa/6)	11	27	P30101-00-01-00	MSMS	41	−1.7	FLQDYFDGNLKR
S18	fibrinogen γ chain precursor (FIBG) (49 kDa/5.8)	7	26	P02679-01-14-00	PMF	42	+3.7	
S19	type II cytoskeletal 4 (CK 4) (57 kDa/6.3)	2	1	P19013-00-01-00	MSMS	56	−2.9	LALDIEIATYR
S20	triosephosphate isomerase (TPIS) (26 kDa/6.5)	6	38	P60175	PMF	45	−3	VPADTEVVCAPPT AYIDFAR

[a] M_r = theoretical molecular mass of the matched protein in kDa; pI = theoretical isoelectric point of the matched protein. [b] Percentage of identified sequence to the complete sequence of known protein. [c] SwissProt accession number. [d] Proteins identified by using MALDI-TOF/TOF-MS through PMF or MALDI-TOF/TOF-MS/MS.

CK 8, and CK 19) were all down-regulated in the MK-treated cells (**Table 1**). Simultaneously, we found that in the MK-treated cells the two glycolytic enzymes, triosephosphate isomerase (TPIS) and non-neural enolase, were co-down-regulated, together with the decrease of ATP synthase β chain (ATPB), which is involved in energy consumption. Another observation corresponding to the enzyme involved in mediating protein interactions was the down-regulation of particularly interesting new cysteine−histidine protein (PINCH) in the MK-treated cells. In contrast, two proteins, annexin A2 (ANX 2) and retinoic acid-binding protein II (RBP II), were up-regulated in the MK-treated cells.

Protein Identification and Expression Confirmation by Western Blotting. Western blotting was performed to verify five selected protein expressions (GSTP1-1, CK 8, CK 18, CK 19, and c-Myc) that may play functional roles in cell proliferation. Among them the c-Myc and CK 18 expressions were not identified on the 2-DE gels in the previous experiments (**Figure**

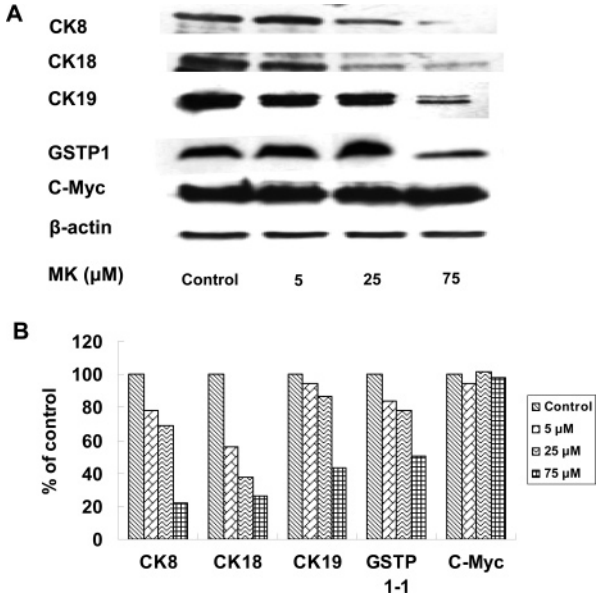

Figure 5. (**A**) 1-D Western blotting analysis of the candidate proteins including CK8, CK18, CK19, GSTP1-1, and c-Myc of Caco-2 cells treated with increasing concentrations of monacolin K for 48 h by using β-actin as internal concentration control and (**B**) densitometrical evaluation of the Western blotting analysis.

3). Western blotting results (**Figure 5**) revealed that the GSTP1-1, CK 8, and CK 19 expressions were down-regulated in a dose-dependent manner during the MK treatment (0−75 μM), which was in agreement with the previous 2-DE results; also another cytoskeletal protein (CK 18) had the same result. On the other hand, c-Myc expression was not regulated in a dose-dependent manner after MK exposure.

DISCUSSION

Proteomics, which aims at characterizing the entire protein complement expressed in cells, can provide direct evidence and complementary information to unravel anti-tumor-specific molecular events during anti-proliferation of cells (*22*). In this study, we first presented the anti-proliferative effect of MK on Caco-2 tumor cells by MTT assay and photomicrographs and used 2-DE-based proteomics to examine the protein profiles of the cells treated with MK for 48 h to identify proteins related to the MK-induced anti-proliferation. Because the mucosal absorption and transepithelial kinetics of nutrients and lipophilic compounds were evaluated using the Caco-2 epithelial colorectal adenocarcinoma cell line, a well-established *in vitro* model to understand nutrient absorption or to assess the physiological response of the intestinal epithelia to antioxidant effects (*16*, *17*), we used this Caco-2 cell line as the model system. Moreover, findings that HMG-CoA reductase promoter activity was several-fold higher in Caco-2 cells than in other normal colon cells suggest that the impacts of sterol-mediated feedback regulation of reductase activity in these tumor cells were enhanced by this increased reductase activity (*23*).

Inhibition of the mevalonate pathway by lovastatin suppresses the syntheses of farnesyl diphosphate and geranylgeranyl diphosphate, the substrates providing the isoprenoid moieties required for the post-translational modification of the cysteine residue in the conserved carboxyl terminus sequence (generally CAAX) of diverse proteins (*24*), some of which have roles in signal transduction (Ras, Rho) and cytoskeletal organization (*7*, *25*, *26*). As a consequence of the lovastatin-imposed depletion of farnesyl and geranylgeranyl diphosphate pools, the essential post-translational processing of intracellular proteins that regulate proliferation is suppressed (*8*, *27*). As in most malignant cells, cell proliferation in intestinal malignancy involves multiple factors (*28*, *29*). It is therefore not surprising that many proteins performing various functional processes were found to be differently expressed between malignant cells and anticancer-agent-treated malignant cells. Here, a total of 17 proteins were uncovered with a more than 1.3-fold altered expression in exposure of Caco-2 cells to 75 μM MK; among them, 15 were down-regulated and two were up-regulated.

First, a group of ROS stress-related enzymes, including PDX 1, 2, and 6 and GSTP1-1, revealed down-regulation in the MK-treated cells (**Table 1**). ROS in cells can affect intracellular redox status. Accumulating evidence has indicated that intracellular redox status plays important roles in gene expression (*30*). It has been suggested that ROS may modulate gene expression through modulating cellular redox status and play roles in all stages of carcinogenesis. PDXs belong to a cysteine-containing antioxidant family of proteins that have been identified from a wide variety of organisms as a scavenger of alkyl hydroperoxides and oxidative radicals (*31*−*33*). In addition to their antioxidant activity, PDXs have been implicated in a number of cellular functions such as cell proliferation and protection of cells from undergoing apoptosis (*34*−*37*). Overexpression of PDXs has been reported in malignant mesothelioma (*32*) and lung carcinomas (*35*). The induction of increased expression of PDXs in breast malignancy was suggested as response to increased production of ROS in carcinomatous tissue (*38*). Cancer cells may become resistant to ROS stress through PDX 1 overexpression (*39*). The down-regulation of three PDXs was induced in the proliferation-inhibited Caco-2 cells after MK exposure in this study, suggesting that PDX isoforms may have some functions unique to the proliferation of Caco-2 cells. Accordingly, in this study the exposure of Caco-2 cells to MK induced co-down-regulation of PDX 1, 2, and 6 in cells, perhaps indicating that MK treatment induced an alteration of tumor cell defense effort in maintaining intracellular homeostasis for cell proliferation.

Furthermore, GSTP1-1 is a member of a large family of GSTs that play an important role in the protection of cells against the toxicity of lipid hydroperoxides generated by oxidative stress (*40*, *41*). Previous studies confirm that GSTP1-1 is highly expressed in most tumor cell lines and is also the dominant GST isoenzyme (*42*). More recent evidence indicated a crucial antiapoptotic role of this enzyme mainly due to its noncovalent binding to c-jun NH_2-terminal kinase (JNK), an enzyme that triggers the apoptotic cascade in the cell (*42*−*44*). In nonstressed cells, GSTP1-1 efficiently inhibits JNK. JNK has been implicated in proapoptotic signaling and may be required for the induced cytotoxicity of a variety of chemotherapy agents (*43*, *45*). Specific GST inhibitors have been shown to cause GSTP1-1 dissociation from the complex and an increase in the JNK activity to enhance the cytotoxic effects of antineoplastic agents (*42*, *43*). In development of *Monascus* food as a functional health food for providing an anticancer effect, our results indicated a MK-induced specific GST inhibitor effect in Caco-2 cells.

CKs are main structural proteins in epithelial cells. They comprise the intermediate filaments of the cytoskeleton and are expressed in various combinations depending on the epithelial type and the degree of differentiation. Overexpression of CK 4, 8, 18, and 19 had been reported in gastric cancer (*46*), colon carcinoma (*47*), and other cancers (*48*−*50*). The functional role of CK 19 was suggested to be associated with apoptosis

prevention in cervical cancer cells (*49*). Furthermore, CK 18 and 19 were reported to be down-regulated and degraded in cleavage during apoptosis of human cholangiocarcinoma cells (*51*) and cleaved by caspases resulting in the reorganization of intermediate filaments during epithelial cell apoptosis (*52*). Inhibition of Ras and Rho farnesylation was originally thought to be the mechanism that mediates statin-induced effects in cancer (*12*−*14*). Rho GTPases play a central role in all eukaryotic cells, coordinately controlling the organization of the actin cytoskeleton with other cellular activities such as cell cycle progression (*7*). It is well-known that proteolysis of cytoskeletal proteins by caspases is a marker of cellular apoptosis (*53*). Furthermore, cytoskeletal actin degradation induced by lovastatin-mediated in cardiomyocytes through the caspase-2 pathway was reported (*54*). Our data indicated a previously unrecognized link between HMG-CoA reductase inhibitor treatment and cytoskeletal protein expression. The results of detected co-down-regulation of CK 4, 8, 18, and 19 in this study perhaps suggest that the reorganization of the intermediate filaments may be induced by MK treatment in Caco-2 cells during the inhibition of cell proliferation. Whether the down-regulated expression levels of these CKs were involved in cleavage of CKs to proteolytic fragments, further investigations are needed to study the proliferation-inhibited effect mediated by MK.

The other three down-regulated proteins were protein disulfide-isomerase (PDI) precursor, protein disulfide-isomerase A3 (PDA 3) precursor, and PINCH (**Table 1**). PDIs are multifunctional redox chaperones in the endoplasmic reticulum (*55*). Due to their ability to catalyze the oxidation, reduction, and isomerization of protein disulfides, PDIs play a role in the regulation of receptor function, cell−cell interaction, and actin filament polymerization (*56*). Their overexpression has been found in human breast ductal carcinoma tissues (*57*). On the other hand, PINCH is an effector of integrin and growth factor signaling, coupling surface receptor to downstream signaling molecules involved in the regulation of cell survival and cell proliferation (*58*, *59*). PINCH was shown to be markedly up-regulated in the tumor-associated stroma of many common cancers (*60*, *61*). Considering these proteins involved in the regulation of cell proliferation, it is reasonable, in this study, that these PDI precursors and PINCH expressions were down-regulated under this MK-induced anti-proliferation in Caco-2 cells. For example, reduced expression of PDI has been found in a nitrosomethyl-urea-induced rat mammary tumor after anticancer treatment (*62*).

Another interesting observation was the down-regulation of the three enzymes ATPB, TPIS, and non-neural enolase. ATPB is involved in cellular energy metabolism, catalyzing ATP production from ADP and inorganic phosphate (*63*). Inhibition of ATP synthase has been reported by angiostatin in blocking tumor angiogenesis *in vivo* (*64*). On the other hand, TPIS and non-neural enolase (two key enzymes of glycolytic pathway) shows increased expression in carcinoma cells (*2*, *65*). The positive correlation of these enzymes may be a reflection of inhibition in glycolysis, reducing energy for the growth of the tumor cells after MK exposure. As stated above, MK treatment in Caco-2 cells perhaps induced an alteration in the tumor cell defense effort. The MK-induced alteration in maintaining defense efforts of the tumor cells may be due to reducing energy supply and respiration rates through decreased expression of these enzymes in metabolism. In contrast, the up-regulation of ANX 2 after MK exposure was another indicator of induction of inhibition in cell proliferation (**Table 1**). ANXs are water-soluble proteins that function as Ca^{2+} channels and regulate membrane fusion (*66*). Although its physiological function *in vivo* is largely unclear currently, *in vitro* ANXs exhibited tumor suppression activities (*67*). ANX 1 and 2 were found to have reduced expressions in many cancers (*68*). However, a previous study suggests that ANX 2 is regulated by cellular redox status and plays a role in the proliferation and metastasis of oxidative stress-induced cancer (*69*).

Lovastatin is currently available for use as effective anticancer therapeutics through blocking the mevalonate biosynthesis pathway, inducing the cancer growth-suppressive actions of isoprenoids, G1 arrest, and apoptosis by altering post-translational processing (farnesylation and geranylgeranylation) of expressed proteins and gene expression. However, red mold rice (containing MK) has been developed into functional health food for use as a human dietary supplement to lower cholesterol level and blood pressure marketed in the United States (Cholestin; Pharmanex, Redwood City, CA). As red mold rice is further developed into functional health food that provides an anticancer effect, a comprehensive and in-depth research of the mechanisms of action in MK that pertain to this anticancer effect should be performed with prospective use in mind. Here, multiple alterations in protein expression were detected in Caco-2 cells after MK exposure. Some of these protein expression alterations were confirmed by Western blotting or correlated with protein expression in some role. Our present findings reflected that the exposure of Caco-2 cells in MK may induce coordinated mediation in cellular function for anti-proliferation in cancer cells and be involved in complicated multiple protein expressions. In this study, induction of cell anti-proliferation in Caco-2 cells after MK exposure involved altered expression of proteins, including peroxiredoxins, cytoskeleton proteins, chaperone proteins, and energy-producing enzymes, among others. We indicated a previously unrecognized link between MK treatment and altered expressions of some redox-related enzymes (PDXs, GSTP1-1, PDIs, and ANX 2). Further combinations of investigation by simultaneously considering these altered protein expressions may provide a focus for future studies to research the mechanisms of action of MK in anti-proliferation in cancer cells while developing red mold rice as a functional health food for anticancer effect.

LITERATURE CITED

(1) Wang, J. J.; Lee, C. L.; Pan, T. M. Improvement of monacolin K, gamma-aminobutyric acid and citrinin production ratio as a function of environmental conditions of *Monascus purpureus* NTU 601. *J. Ind. Microbiol. Biotechnol.* **2003**, *30*, 669−676.

(2) Chen, F.; Hu, X. Study on red fermented rice with high concentration of monacolin K and low concentration of citrinin. *Int. J. Food Microbiol.* **2005**, *103*, 331−337.

(3) Lee, H.; Park, H.; Kim, Y. J.; Kim, H. J.; Ahn, Y. M.; Park, B.; Park, J. H.; Lee, B. E. Expression of lectin-like oxidized low-density lipoprotein receptor-1 (LOX-1) in human preeclamptic placenta: possible implications in the process of trophoblast apoptosis. *Placenta* **2005**, *26*, 226−233.

(4) Tanaka, T.; Akatsuka, S.; Ozeki, M.; Shirase, T.; Hiai, H.; Toyokuni, S. Redox regulation of annexin 2 and its implications for oxidative stress-induced renal carcinogenesis and metastasis. *Oncogene* **2004**, *23*, 3980−3989.

(5) Shepherd, J.; Blauw, G. J.; Murphy, M. B.; Bollen, E. L.; Buckley, B. M.; Cobbe, S. M.; Ford, I.; Gaw, A.; Hyland, M.; Jukema, J. W.; Kamper, A. M.; Macfarlane, P. W.; Meinders, A. E.; Norrie, J.; Packard, C. J.; Perry, I. J.; Stott, D. J.; Sweeney, B. J.; Twomey, C.; Westendorp, R. G. Pravastatin in elderly individuals at risk of vascular disease (PROSPER): a randomised controlled trial. *Lancet* **2002**, *360*, 1623−1630.

(6) Johnson, T. E.; Zhang, X.; Bleicher, K. B.; Dysart, G.; Loughlin, A. F.; Schaefer, W. H.; Umbenhauer, D. R. Statins induce apoptosis in rat and human myotube cultures by inhibiting protein geranylgeranylation but not ubiquinone. *Toxicol. Appl. Pharmacol.* **2004**, *200*, 237−250.
(7) Etienne-Manneville, S.; Hall, A. Rho GTPases in cell biology. *Nature* **2002**, *420*, 629−635.
(8) Mackay, D. J.; Hall, A. Rho GTPases. *J Biol. Chem.* **1998**, *273*, 20685−20688.
(9) Bhattacharya, M.; Babwah, A. V.; Ferguson, S. S. Small GTP-binding protein-coupled receptors. *Biochem. Soc. Trans.* **2004**, *32*, 1040−1044.
(10) Hippenstiel, S.; Kratz, T.; Krull, M.; Seybold, J.; von Eichel-Streiber, C.; Suttorp, N. Rho protein inhibition blocks protein kinase C translocation and activation. *Biochem. Biophys. Res. Commun.* **1998**, *245*, 830−834.
(11) Su, Y. C.; Wang, J. J.; Lin, T. T.; Pan, T. M. Production of the secondary metabolites gamma-aminobutyric acid and monacolin K by *Monascus J. Ind. Microbiol. Biotechnol.* **2003**, *30*, 41−46.
(12) Cafforio, P.; Dammacco, F.; Gernone, A.; Silvestris, F. Statins activate the mitochondrial pathway of apoptosis in human lymphoblasts and myeloma cells. *Carcinogenesis* **2005**, *26*, 883−891.
(13) Graaf, M. R.; Richel, D. J.; van Noorden, C. J.; Guchelaar, H. J. Effects of statins and farnesyltransferase inhibitors on the development and progression of cancer. *Cancer Treat. Rev.* **2004**, *30*, 609−641.
(14) Tojo, Y.; Bandoh, S.; Fujita, J.; Kubo, A.; Ishii, T.; Fukunaga, Y.; Ueda, Y.; Yang, Y.; Wu, F.; Huang, C. L.; Yokomise, H.; Ishida, T. Aberrant messenger RNA splicing of the cytokeratin 8 in lung cancer. *Lung Cancer* **2003**, *42*, 153−161.
(15) Gagnaire, V.; Piot, M.; Camier, B.; Vissers, J. P.; Jan, G.; Leonil, J. Survey of bacterial proteins released in cheese: a proteomic approach. *Int. J. Food Microbiol.* **2004**, *94*, 185−201.
(16) Konishi, Y.; Hitomi, Y.; Yoshida, M.; Yoshioka, E. Absorption and bioavailability of artepillin C in rats after oral administration. *J. Agric. Food Chem.* **2005**, *53*, 9928−9933.
(17) Tarozzi, A.; Hrelia, S.; Angeloni, C.; Morroni, F.; Biagi, P.; Guardigli, M.; Cantelli-Forti, G.; Hrelia, P. Antioxidant effectiveness of organically and non-organically grown red oranges in cell culture systems. *Eur. J. Nutr.* **2006**, *45*, 152−158.
(18) Gerlier, D.; Thomasset, N. Use of MTT colorimetric assay to measure cell activation. *J. Immunol. Methods* **1986**, *94*, 57−63.
(19) Mosmann, T. Rapid colorimetric assay for cellular growth and survival: application to proliferation and cytotoxicity assays. *J. Immunol. Methods* **1983**, *65*, 55−63.
(20) Larner, J.; Jane, J.; Laws, E.; Packer, R.; Myers, C.; Shaffrey, M. A phase I-II trial of lovastatin for anaplastic astrocytoma and glioblastoma multiforme. *Am. J. Clin. Oncol.* **1998**, *21*, 579−583.
(21) Lee, C. L.; Tsai, T. Y.; Wang, J. J.; Pan, T. M. In vivo hypolipidemic effects and safety of low dosage Monascus powder in a hamster model of hyperlipidemia. *Appl. Microbiol. Biotechnol.* **2006**, *70*, 533−540.
(22) Skalnikova, H.; Halada, P.; Dzubak, P.; Hajduch, M.; Kovarova, H. Protein fingerprints of anti-cancer effects of cyclin-dependent kinase inhibition: identification of candidate biomarkers using 2-D liquid phase separation coupled to mass spectrometry. *Technol. Cancer Res. Treat.* **2005**, *4*, 447−454.
(23) Hentosh, P.; Yuh, S. H.; Elson, C. E.; Peffley, D. M. Sterol-independent regulation of 3-hydroxy-3-methylglutaryl coenzyme A reductase in tumor cells. *Mol. Carcinog.* **2001**, *32*, 154−166.
(24) Hancock, J. F.; Magee, A. I.; Childs, J. E.; Marshall, C. J. All ras proteins are polyisoprenylated but only some are palmitoylated. *Cell* **1989**, *57*, 1167−1177.
(25) Cau, J.; Hall, A. Cdc42 controls the polarity of the actin and microtubule cytoskeletons through two distinct signal transduction pathways. *J. Cell Sci.* **2005**, *118*, 2579−2587.
(26) Hall, A. Rho GTPases and the actin cytoskeleton. *Science* **1998**, *279*, 509−514.
(27) Mo, H.; Elson, C. E. Studies of the isoprenoid-mediated inhibition of mevalonate synthesis applied to cancer chemotherapy and chemoprevention. *Exp. Biol. Med. (Maywood)* **2004**, *229*, 567−585.
(28) Alfonso, P.; Nunez, A.; Madoz-Gurpide, J.; Lombardia, L.; Sanchez, L.; Casal, J. I. Proteomic expression analysis of colorectal cancer by two-dimensional differential gel electrophoresis. *Proteomics* **2005**, *5*, 2602−2611.
(29) Turck, N.; Richert, S.; Gendry, P.; Stutzmann, J.; Kedinger, M.; Leize, E.; Simon-Assmann, P.; Van Dorsselaer, A.; Launay, J. F. Proteomic analysis of nuclear proteins from proliferative and differentiated human colonic intestinal epithelial cells. *Proteomics* **2004**, *4*, 93−105.
(30) Savaraj, N.; Wei, Y.; Unate, H.; Liu, P. M.; Wu, C. J.; Wangpaichitr, M.; Xia, D.; Xu, H. J.; Hu, S. X.; Tien Kuo, M. Redox regulation of matrix metalloproteinase gene family in small cell lung cancer cells. *Free Radical Res.* **2005**, *39*, 373−381.
(31) Henkle-Duhrsen, K.; Kampkotter, A. Antioxidant enzyme families in parasitic nematodes. *Mol. Biochem. Parasitol.* **2001**, *114*, 129−142.
(32) Kinnula, V. L.; Lehtonen, S.; Sormunen, R.; Kaarteenaho-Wiik, R.; Kang, S. W.; Rhee, S. G.; Soini, Y. Overexpression of peroxiredoxins I, II, III, V, and VI in malignant mesothelioma. *J. Pathol.* **2002**, *196*, 316−323.
(33) Hirotsu, S.; Hakoshima, T.; Abe, Y.; Nishino, T. Structural basis of peroxiredoxin functions: a new antioxidant protein family scavenging reactive oxygen species. *Tanpakushitsu Kakusan Koso* **2000**, *45*, 2463−2474.
(34) Immenschuh, S.; Baumgart-Vogt, E. Peroxiredoxins, oxidative stress, and cell proliferation. *Antioxid. Redox Signaling* **2005**, *7*, 768−777.
(35) Lehtonen, S. T.; Svensk, A. M.; Soini, Y.; Paakko, P.; Hirvikoski, P.; Kang, S. W.; Saily, M.; Kinnula, V. L. Peroxiredoxins, a novel protein family in lung cancer. *Int. J. Cancer* **2004**, *111*, 514−521.
(36) Oh, S. T.; Seo, J. S.; Moon, U. Y.; Kang, K. H.; Shin, D. J.; Yoon, S. K.; Kim, W. H.; Park, J. G.; Lee, S. K. A naturally derived gastric cancer cell line shows latency I Epstein-Barr virus infection closely resembling EBV-associated gastric cancer. *Virology* **2004**, *320*, 330−336.
(37) Nonn, L.; Berggren, M.; Powis, G. Increased expression of mitochondrial peroxiredoxin-3 (thioredoxin peroxidase-2) protects cancer cells against hypoxia and drug-induced hydrogen peroxide-dependent apoptosis. *Mol. Cancer Res.* **2003**, *1*, 682−689.
(38) Karihtala, P.; Mantyniemi, A.; Kang, S. W.; Kinnula, V. L.; Soini, Y. Peroxiredoxins in breast carcinoma. *Clin. Cancer Res.* **2003**, *9*, 3418−3424.
(39) Maeda, T.; Matsunuma, A.; Kurahashi, I.; Yanagawa, T.; Yoshida, H.; Horiuchi, N. Induction of osteoblast differentiation indices by statins in MC3T3-E1 cells. *J. Cell. Biochem.* **2004**, *92*, 458−471.
(40) Allen, S.; Heath, P. R.; Kirby, J.; Wharton, S. B.; Cookson, M. R.; Menzies, F. M.; Banks, R. E.; Shaw, P. J. Analysis of the cytosolic proteome in a cell culture model of familial amyotrophic lateral sclerosis reveals alterations to the proteasome, antioxidant defenses, and nitric oxide synthetic pathways. *J. Biol. Chem.* **2003**, *278*, 6371−6383.
(41) Cookson, M. S.; Reuter, V. E.; Linkov, I.; Fair, W. R. Glutathione S-transferase PI (GST-pi) class expression by immunohistochemistry in benign and malignant prostate tissue. *J. Urol.* **1997**, *157*, 673−676.
(42) McIlwain, C. C.; Townsend, D. M.; Tew, K. D. Glutathione S-transferase polymorphisms: cancer incidence and therapy. *Oncogene* **2006**, *25*, 1639−1648.
(43) Guo, Y. S.; Jin, G. F.; Houston, C. W.; Thompson, J. C.; Townsend, C. M., Jr. Insulin-like growth factor-I promotes multidrug resistance in MCLM colon cancer cells. *J. Cell. Physiol.* **1998**, *175*, 141−148.

(44) Turella, P.; Cerella, C.; Filomeni, G.; Bullo, A.; De Maria, F.; Ghibelli, L.; Ciriolo, M. R.; Cianfriglia, M.; Mattei, M.; Federici, G.; Ricci, G.; Caccuri, A. M. Proapoptotic activity of new glutathione S-transferase inhibitors. *Cancer Res.* **2005**, *65*, 3751−3761.

(45) Yin, Z.; Ivanov, V. N.; Habelhah, H.; Tew, K.; Ronai, Z. Glutathione S-transferase p elicits protection against H_2O_2-induced cell death via coordinated regulation of stress kinases. *Cancer Res.* **2000**, *60*, 4053−4057.

(46) Kim, S.; Wong, P.; Coulombe, P. A. A keratin cytoskeletal protein regulates protein synthesis and epithelial cell growth. *Nature* **2006**, *441*, 362−365.

(47) Pantel, K.; Dickmanns, A.; Zippelius, A.; Klein, C.; Shi, J.; Hoechtlen-Vollmar, W.; Schlimok, G.; Weckermann, D.; Oberneder, R.; Fanning, E.; et al. Establishment of micrometastatic carcinoma cell lines: a novel source of tumor cell vaccines. *J. Natl. Cancer Inst.* **1995**, *87*, 1162−1168.

(48) Ferrer, A.; Marce, S.; Bellosillo, B.; Villamor, N.; Bosch, F.; Lopez-Guillermo, A.; Espinet, B.; Sole, F.; Montserrat, E.; Campo, E.; Colomer, D. Activation of mitochondrial apoptotic pathway in mantle cell lymphoma: high sensitivity to mitoxantrone in cases with functional DNA-damage response genes. *Oncogene* **2004**, *23*, 8941−8949.

(49) Yinghao, Z.; Jun, W.; Yuanbo, C.; Jiachang, Y.; Xiaohong, F. Rotary torque produced by proton motive force in FoF1 motor. *Biochem. Biophys. Res. Commun.* **2005**, *331*, 370−374.

(50) Copete, M. A.; Wendt, K.; Chen, S. Y. Expression of p53, Ki-67 and cytokeratin-4 (CK4) in oral papillomas. *J. Oral Pathol. Med.* **1997**, *26*, 211−216.

(51) Svasti, J.; Srisomsap, C.; Subhasitanont, P.; Keeratichamroen, S.; Chokchaichamnankit, D.; Ngiwsara, L.; Chimnoi, N.; Pisutjaroenpong, S.; Techasakul, S.; Chen, S. T. Proteomic profiling of cholangiocarcinoma cell line treated with pomiferin from *Derris malaccensis*. *Proteomics* **2005**, *5*, 4504−4509.

(52) Vanoverberghe, K.; Vanden Abeele, F.; Mariot, P.; Lepage, G.; Roudbaraki, M.; Bonnal, J. L.; Mauroy, B.; Shuba, Y.; Skryma, R.; Prevarskaya, N. Ca^{2+} homeostasis and apoptotic resistance of neuroendocrine-differentiated prostate cancer cells. *Cell Death Differ.* **2004**, *11*, 321−330.

(53) Bursch, W.; Hochegger, K.; Torok, L.; Marian, B.; Ellinger, A.; Hermann, R. S. Autophagic and apoptotic types of programmed cell death exhibit different fates of cytoskeletal filaments. *J. Cell Sci.* **2000**, *113* (Pt 7), 1189−1198.

(54) Kong, J. Y.; Rabkin, S. W. Cytoskeletal actin degradation induced by lovastatin in cardiomyocytes is mediated through caspase-2. *Cell Biol. Int.* **2004**, *28*, 781−790.

(55) Saadi-Kheddouci, S.; Berrebi, D.; Romagnolo, B.; Cluzeaud, F.; Peuchmaur, M.; Kahn, A.; Vandewalle, A.; Perret, C. Early development of polycystic kidney disease in transgenic mice expressing an activated mutant of the beta-catenin gene. *Oncogene* **2001**, *20*, 5972−5981.

(56) Noiva, R. Protein disulfide isomerase: the multifunctional redox chaperone of the endoplasmic reticulum. *Semin. Cell Dev. Biol.* **1999**, *10*, 481−493.

(57) Bini, L.; Magi, B.; Marzocchi, B.; Arcuri, F.; Tripodi, S.; Cintorino, M.; Sanchez, J. C.; Frutiger, S.; Hughes, G.; Pallini, V.; Hochstrasser, D. F.; Tosi, P. Protein expression profiles in human breast ductal carcinoma and histologically normal tissue. *Electrophoresis* **1997**, *18*, 2832−2841.

(58) Fukuda, T.; Chen, K.; Shi, X.; Wu, C. PINCH-1 is an obligate partner of integrin-linked kinase (ILK) functioning in cell shape modulation, motility, and survival. *J. Biol. Chem.* **2003**, *278*, 51324−51333.

(59) Biven, K.; Erdal, H.; Hagg, M.; Ueno, T.; Zhou, R.; Lynch, M.; Rowley, B.; Wood, J.; Zhang, C.; Toi, M.; Shoshan, M. C.; Linder, S. A novel assay for discovery and characterization of pro-apoptotic drugs and for monitoring apoptosis in patient sera. *Apoptosis* **2003**, *8*, 263−268.

(60) Gao, J.; Arbman, G.; Rearden, A.; Sun, X. F. Stromal staining for PINCH is an independent prognostic indicator in colorectal cancer. *Neoplasia* **2004**, *6*, 796−801.

(61) Wang-Rodriguez, J.; Dreilinger, A. D.; Alsharabi, G. M.; Rearden, A. The signaling adapter protein PINCH is up-regulated in the stroma of common cancers, notably at invasive edges. *Cancer* **2002**, *95*, 1387−1395.

(62) Charrier, L.; Jarry, A.; Toquet, C.; Bou-Hanna, C.; Chedorge, M.; Denis, M.; Vallette, G.; Laboisse, C. L. Growth phase-dependent expression of ICAD-L/DFF45 modulates the pattern of apoptosis in human colonic cancer cells. *Cancer Res.* **2002**, *62*, 2169−2174.

(63) Al-Shawi, M. K.; Ketchum, C. J.; Nakamoto, R. K. Energy coupling, turnover, and stability of the F0F1 ATP synthase are dependent on the energy of interaction between gamma and beta subunits. *J. Biol. Chem.* **1997**, *272*, 2300−2306.

(64) Roth, G. A.; Krenn, C.; Brunner, M.; Moser, B.; Ploder, M.; Spittler, A.; Pelinka, L.; Sautner, T.; Wolner, E.; Boltz-Nitulescu, G.; Ankersmit, H. J. Elevated serum levels of epithelial cell apoptosis-specific cytokeratin 18 neoepitope m30 in critically ill patients. *Shock* **2004**, *22*, 218−220.

(65) Yang, W. L.; Addona, T.; Nair, D. G.; Qi, L.; Ravikumar, T. S. Apoptosis induced by cryo-injury in human colorectal cancer cells is associated with mitochondrial dysfunction. *Int. J. Cancer* **2003**, *103*, 360−369.

(66) Balcerzak, M.; Hamade, E.; Zhang, L.; Pikula, S.; Azzar, G.; Radisson, J.; Bandorowicz-Pikula, J.; Buchet, R. The roles of annexins and alkaline phosphatase in mineralization process. *Acta Biochim. Pol.* **2003**, *50*, 1019−1038.

(67) Liu, Z. L.; Luo, J. M.; Dong, Z. R.; Wang, F. X.; Zhang, X. J.; Yang, J. C.; Du, X. Y.; Yao, L. In vitro effects of mevastatin on the proliferation and apoptosis in human multiple myeloma cell line U266. *Zhongguo Shi Yan Xue Ye Xue Za Zhi* **2004**, *12*, 340−345.

(68) Lehnigk, U.; Zimmermann, U.; Woenckhaus, C.; Giebel, J. Localization of annexins I, II, IV and VII in whole prostate sections from radical prostatectomy patients. *Histol. Histopathol.* **2005**, *20*, 673−680.

(69) Caplan, J. F.; Filipenko, N. R.; Fitzpatrick, S. L.; Waisman, D. M. Regulation of annexin A2 by reversible glutathionylation. *J. Biol. Chem.* **2004**, *279*, 7740−7750.

Received for review April 15, 2006. Revised manuscript received June 26, 2006. Accepted June 27, 2006.

JF061060C